Journal of Cleaner Production 373 (2022) 133546

Contents lists available at ScienceDirect

Journal of Cleaner Production

journal homepage: www.elsevier.com/locate/jclepro

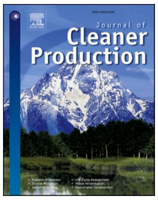

Achieving low-carbon cementitious materials with high mechanical properties using $CaCO_3$ suspension produced by CO_2 sequestration

Zhuo Liu, Jiang Du, Weina Meng [*]

Department of Civil, Environmental, and Ocean Engineering, Stevens Institute of Technology, 614 River Terrace, Hoboken, NJ, 07030, United States

ARTICLE INFO

Handling Editor: Prof. Jiri Jaromir Klemeš

Keywords:
CO_2 utilization
Carbon footprint
Low-carbon cementitious materials
$CaCO_3$
Sustainable civil infrastructure

ABSTRACT

High carbon emissions of cementitious materials is increasingly raising concerns under the grand goal of global carbon neutrality. This paper presents an approach to achieve low-carbon cementitious materials and enhance the mechanical properties while retaining the desired constructability for cast-in-place and precast applications of civil infrastructure. The proposed approach utilizes CO_2 to produce a $CaCO_3$ suspension that is uniformly dispersed and used to prepare cement pastes. The mechanical properties were tested, and the results showed that the 28-day compressive strength was increased by up to 16%. Further research was conducted to understand the effects of $CaCO_3$ suspension on cement hydration kinetics and microstructures of cement pastes through isothermal calorimetry, thermal gravimetry analysis, mercury intrusion porosimetry, dynamic light scattering analyzer, and scanning electron microscopy. The results revealed that the $CaCO_3$ suspension promoted cement hydration and densified the microstructures because of the nucleation effect caused by the high-level dispersion of $CaCO_3$ particles. The proposed approach provides an alternative solution for CO_2 utilization in the concrete industry with minimal modification of the manufacturing facility and offers a promising avenue for achieving low-carbon infrastructure.

1. Introduction

The production of concrete involves significant carbon emissions. According to previous research (Karl and Trenberth, 2003; Ritchie and Roser, 2020), manufacturing 1 ton of cement releases 0.8 tons of carbon dioxide (CO_2) (Bodansky, 2016). In 2020, the cement industry handles about 7% of annual carbon emissions (Zhang et al., 2020a). Climate change causes many serious problems, such as sea-level rise, extreme temperature and precipitation, and frequent wildfires that endanger the safety of the public and the wealth of the economy (Lempert et al., 2019; Salvia et al., 2021). The Paris Agreement set a goal to limit the temperature increase to 1.5 °C by 2050 (Di Maria et al., 2020). China announced that it would achieve peak carbon emissions in 2030 and carbon neutrality in 2060 (Hepburn et al., 2019); the United States planned to achieve carbon neutrality in 2050 (Schreyer et al., 2020), and many other countries planned to achieve carbon neutrality around 2050 (Østergaard et al., 2020; Zhang et al., 2020b). To achieve carbon neutrality, different pathways have been proposed, such as reduction of carbon emissions by adopting renewable energy (Godin et al., 2021a), storage of carbon via geological (Raza et al., 2019a) and biological systems (Stuardi et al., 2019), and utilization of carbon dioxide (CO_2) for valuable industrial products (Norhasyima and Mahlia, 2018; Godin et al., 2021b).

Previous research showed that CO_2 could be stored in concrete via a mineralization process (Ho et al., 2021; Raza et al., 2019b; Zhang et al., 2020c). This is interesting because of the large volume and long service life of concrete in civil infrastructure. Basically, CO_2 reacts with cement and cement hydration products, such as calcium hydroxide, producing calcium carbonate ($CaCO_3$), which is chemically and physically stable under ambient conditions. This mineralization process is known as “carbonation,” which naturally occurs at a low rate within concrete and is recognized as a deterioration factor in concrete structures because this process reduces the pH value and tends to promote corrosion of reinforcement (Qian et al., 2018). Due to the slow reaction rate, spontaneous carbonation makes limited contributions to the carbon neutrality goal. Recent research has shown that it is possible to use high-purity CO_2 to increase the reaction rate and enhance the compressive strengths and durability of concrete (Ho et al., 2021; Raza et al., 2019b). In this regard, existing approaches can be categorized into three main groups according to the stages of concrete production. The first group of approaches

---

[*] Corresponding author.
E-mail address: weina.meng@stevens.edu (W. Meng).

https://doi.org/10.1016/j.jclepro.2022.133546
Received 9 February 2022; Received in revised form 3 August 2022; Accepted 5 August 2022
Available online 10 August 2022

sequesters CO_2 using solid wastes, such as recycled concrete aggregate (Lu et al., 2019) and steel slag (Ashraf, 2016), before mixing. The wastes contain metal oxides, such as CaO and MgO, which react with CO_2 to generate carbonates (Šavija and Luković, 2016). The treated waste is used to prepare concrete that permanently locks CO_2 inside. However, the treatment reduces the mechanical strength and chemical stability of some types of wastes, depending on the chemical composition and the physical properties that vary from different sources (Chen and Gao, 2019). Some types of solid wastes cause internal sulfate attacks (Pan et al., 2017) or leach toxic chemicals to the environment (Ashraf et al., 2019). The second group of approaches uses CO_2 to cure fresh concrete in CO_2-rich environments (Liu and Meng, 2021). The concentration of CO_2 and pressure are kept high to let CO_2 dissolve into water and react with cement to form dense carbonates on a thin surface of concrete (Monkman and MacDonald, 2017). However, this method is mainly applied to precast concrete because it is inconvenient and costly to build a CO_2-rich and high-pressure chamber to accommodate cast-in-place structures. Additionally, the mineralization rate is low. The presence of formwork further compromises the reaction rate by hindering the diffusion of CO_2 into concrete. The third group injects gaseous or liquid CO_2 into fresh concrete during mixing (Monkman et al., 2016). The injected CO_2 dissolves in the mixing water and reacts with the cement to produce $CaCO_3$. However, the amount of sequestered CO_2 is low, typically less than 0.3% of the mass of cement (Monkman and MacDonald, 2016), due to the low dissolvability of CO_2 in water, low concentrations of alkalis in fresh concrete, and the low reaction rate between CO_2 and alkali (Kawashima et al., 2013). Special facilities are also required for mixing to prevent the release of unreacted CO_2 into the ambient atmosphere (Raki et al., 2010).

This research proposes an alternative approach to utilize CO_2 to prepare low-carbon cementitious materials with multiple advantages over the existing approaches: (1) high CO_2 sequestration efficiency and reaction rates, (2) high mechanical properties, and (3) availability for cast-in-place and precast concrete applications. Specifically, the proposed approach involves two main processes. The first process is the production of $CaCO_3$ suspension by injecting gaseous CO_2 into $Ca(OH)_2$ solutions. The second is the production of low-carbon cementitious materials through the normal mixing process and the incorporation of the $CaCO_3$ suspension. Both processes are compatible with existing industrial facilities and convenient for large-scale production. The CO_2 injection method has been adopted to manufacture $CaCO_3$ in chemical and metallurgical industries (Yang and Che, 2018; Su et al., 2016) because the reaction rate is high and controllable (Kawashima et al., 2014; Liew et al., 2019; Batuecasa et al., 2021). It is envisioned that the proposed approach will be applied to realistic applications for both precast and cast-in-place construction. The proposed approach does not require a high-concentration CO_2 source. Since CO_2 is used to produce inert $CaCO_3$ particles, which do not affect the pH value, before concrete mixing, the proposed approach likely retains the corrosion-resistant layer of steel and the durability of concrete structures.

Based on the literature review, multiple knowledge gaps have been identified. First, the effect of the $CaCO_3$ suspension on the key properties of cementitious materials is unknown. Previous research showed that the use of $CaCO_3$ particles in cementitious materials compromised flowability, compressive strength, and durability due to agglomeration when the dosage was higher than 3% (Yeşilmen et al., 2015; Han et al., 2011). There is a lack of knowledge about the effect of the $CaCO_3$ suspension produced with the proposed approach. Second, the sizes of $CaCO_3$ particles in the suspension and their level of dispersion are unknown. Because particle size affects the hydration reactions and microstructures of cementitious materials, it is important to know the particle sizes and level of dispersion. Previous research showed that uniform dispersion of nanoparticles increased the compressive strength of cementitious materials (Liu et al., 2015; Wu et al., 2018; Camiletti et al., 2013), but it is a major technical challenge to uniformly disperse nanomaterials that are generally prone to agglomeration. Agglomeration limits the volume of nanomaterials and significantly compromises the mechanical strengths and durability of cementitious materials (Xu et al., 2017). Third, the effect of the $CaCO_3$ suspension on the life-cycle carbon footprint is unclear. It is hypothesized that the proposed method produces a well-dispersed $CaCO_3$ suspension. It is further posited that the well-dispersed $CaCO_3$ suspension improves the key properties and life-cycle performance of low-carbon cementitious materials.

To address the abovementioned knowledge gaps, the main objectives of this paper are to (1) investigate the effects of the $CaCO_3$ suspension on the flowability, compressive strength, and microstructures of cementitious materials, and investigate the mechanisms of these effects. To this end, experiments were conducted to prepare, test, and characterize the $CaCO_3$ suspension and cement paste. This research develops processing methods available for upscale manufacturing to increase the carbon sequestration rate and improve the key properties of low-carbon cementitious materials. The performance of the use of $CaCO_3$ suspension is compared with the use of nano-$CaCO_3$ powder that is mixed with mixing water for cement paste mixing in terms of the flowability and mechanical properties of cement paste. The underlying mechanisms were investigated by evaluating the particle size distribution and dispersion of $CaCO_3$, as well as the effects on cement hydration kinetics and microstructures of cement paste via dynamic light scattering, scanning electron microscopy-energy dispersive X-ray spectroscopy (SEM-EDS), isothermal calorimetry, thermal gravimetry analysis (TGA), and mercury intrusion porometer (MIP). This research advances the development of low-carbon concrete for sustainable civil infrastructure.

2. Materials and experimental program

2.1. Raw materials

Type I Portland cement was adopted to prepare the cement paste. The chemical composition of the cement is shown in Table 1. Hydrated lime with a purity of 99.2% was used to prepare the $Ca(OH)_2$ suspension. Gaseous CO_2 with a purity of 100% was adopted in this research to avoid the inclusion of other variables. For comparison, commercial nano-$CaCO_3$ powder with a purity of higher than 97.5% and particle sizes in the range of 30–60 nm was investigated, the typical properties of the nano-$CaCO_3$ powder are presented in Table 2. A polycarboxylate-based high-range water reducer (HRWR) was used to improve the flowability of the mixtures.

2.2. Preparation of $CaCO_3$ suspension

$CaCO_3$ suspension is a mixture of $CaCO_3$ particles and water (see Fig. 1). Two methods were used to prepare $CaCO_3$ suspensions. The first method is an injection method, denoted by CI, which injects CO_2 gas into $Ca(OH)_2$ solution to synthesize $CaCO_3$. The second is a mixing method, denoted by CP, which mixes the commercial nano-$CaCO_3$ powder with water and stirs the mixture for the dispersion of the particles. Regarding the CI method, to prepare a $CaCO_3$ with a target concentration, the required $Ca(OH)_2$ concentration according to Eq. (1) was calculated. Then the $Ca(OH)_2$ solution with calculated concentration was prepared and then fully carbonated by CO_2 injection process. During CO_2 injection, CO_2 was injected into $Ca(OH)_2$ suspensions using a gas injector, as shown in Fig. 2. The gas flow rate was controlled at 30 L/min using a flow meter. An air stone was used to disperse CO_2. The injection of CO_2 was continued until the mass of the suspension became stable, indicating that no more CO_2 was absorbed. The injection of CO_2 consumed $Ca(OH)_2$ and produced $CaCO_3$. The final CO_2 absorption degree of $Ca(OH)_2$, which refers to the ratio of the final CO_2 absorption to the maximum theoretical CO_2 absorption, depends on the $Ca(OH)_2$ concentration. Preliminary studies showed that the CO_2 absorption degree was lower than 100% when the concentration of $Ca(OH)_2$ suspension exceeded 1.5%. To fully carbonate $Ca(OH)_2$ suspension with

Table 1
Chemical composition of Type I Portland cement (%).

SiO_2	Al_2O_3	Fe_2O_3	CaO	MgO	SO_3	Na_2O.	K_2O	TiO_2	P_2O_5	Mn_2O_3	LOI
22.44	2.76	2.24	68.05	0.91	2.25	0.19	0.11	0.14	0.09	0.03	1.28

Table 2
Properties of nano-$CaCO_3$ powder.

Particle size	Bulk density	pH	Moisture content	$CaCO_3$ content	MgO content
30–60 nm	0.68 g/ml	8.0–9.0	0.5%	>97.5%	<0.5%

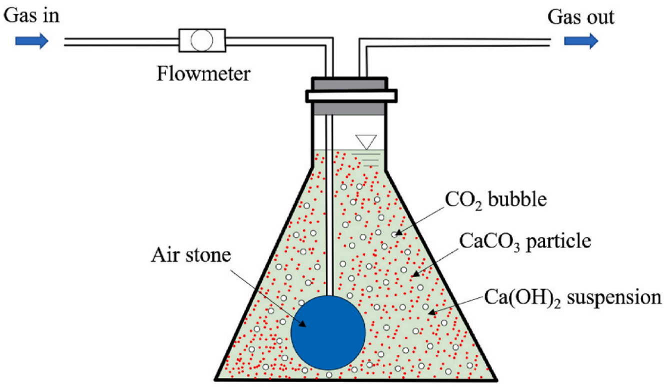

Fig. 1. Illustration of the preparation of $CaCO_3$ suspension by injecting CO_2 into $Ca(OH)_2$.

concentrations higher than 1.5%, a three-step procedure is proposed: (1) dilute the $Ca(OH)_2$ concentration to 1.5% by adding deionized water, (2) inject CO_2 to achieve a maximum CO_2 absorption, and (3) remove the upper layer water using a syringe after precipitation of $CaCO_3$. This procedure was followed to prepare high concentrations of nano-$CaCO_3$ suspension (2%, 4%, and 6%).

$$Ca(OH)_2+CO_2\rightarrow CaCO_3+H_2O \qquad \text{Eq. (1)}$$

2.3. *Mixture design and sample preparation*

The investigated mixtures are listed in Table 3. The control mixture was prepared by mixing the cement with tap water. Mixtures CI-0.5%, CI-1%, CI-2%, CI-4%, and CI-6% are the mixtures prepared using $CaCO_3$ suspensions with concentrations of 0.5%, 1%, 2%, 4%, and 6%, respectively, prepared using the CI method. Specifically, mixtures CI-0.5% and CI-1% were directly produced by CO_2 injection, and mixtures CI-2%, CI-4%, and CI-6% were prepared by the dilution-injection-separation method, as elaborated in Section 2.2. Mixtures CP-1%, CP-2%, CP-4%, and CP-6% are mixtures prepared using $CaCO_3$ suspensions with concentrations of 1%, 2%, 4%, and 6%, respectively, prepared using the CP method. The cement and $CaCO_3$ were considered binders, and the water-to-binder ratio (w/b) was fixed at 0.4 for all investigated mixtures.

The cement and the prepared $CaCO_3$ suspensions were added to a Hobart mixer with a volume capacity of 19 L and mixed for 5 min at a constant rotating rate (2 rps) before casting the specimens. The specimens were then cast using molds placed on a vibration table. Immediately after cement paste casting, the specimens were covered with wet burlap and plastic sheets to maintain moisture. The specimens were demolded after 1 day and then cured in lime-saturated water at room temperature (23 ± 2 °C) until testing.

2.4. *Experimental testing*

2.4.1. *Fresh and hardened properties*

The mini-slump spread was measured according to ASTM C230/C230M. The compressive strength at 1, 7, and 28 days was evaluated using 50 mm cubes, according to ASTM C109. The loading rate was kept at 1.8 kN/min.

2.4.2. *Heat of hydration*

The hydration heat was measured using an isothermal calorimeter (Model: Calmetrix I-Cal 4000 HPC) to evaluate the hydration kinetics. Approximately 60 g of fresh cementitious suspension was sealed in a plastic vial and placed into the calorimeter, which was maintained at 25 °C. The heat of hydration was constantly measured from 2 min after completion of mixing to 48 h. The results were normalized by the mass

Table 3
The investigated mixtures (unit: g).

Designation	Cement	In-situ produced $CaCO_3$	Nano-$CaCO_3$ powder	Water	HRWR
Control	1000	0	–	400	2.5
CI-0.5%	998	2	–	400	2.5
CI-1%	996	4	–	400	2.5
CI-2%	992	8	–	400	2.5
CI-4%	984	16	–	400	2.5
CI-6%	976	24	–	400	2.5
CP-1%	996	–	4	400	2.5
CP-2%	992	–	8	400	2.5
CP-4%	984	–	16	400	2.5
CP-6%	976	–	24	400	2.5

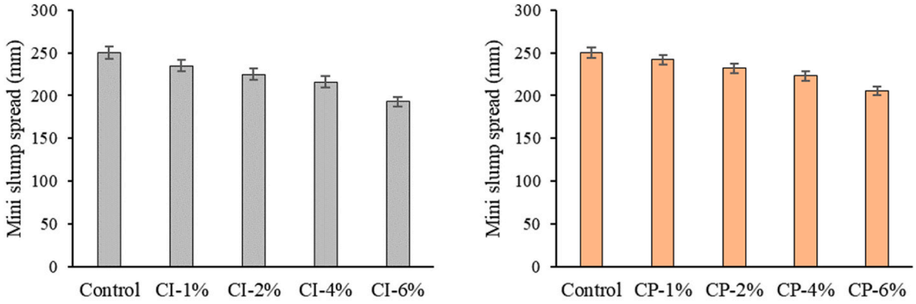

(a) (b)

Fig. 2. Mini-slump spread of the investigated mixtures prepared with (a) CI-produced $CaCO_3$ suspensions and (b) CP-produced $CaCO_3$ suspensions.

of the binder.

2.4.3. *Thermogravimetry analysis*

The hydration products of investigated mixtures were evaluated using a thermogravimetric analyzer (model: TA® TG55). About 50 mg of the sample from dried slices was crushed into fine powders and vacuum dried for 24 h before the test. During the test, the sample was heated at a constant rate of 20 °C/min from 20 °C to 1000 °C in a nitrogen flow at a constant flow rate of 50 ml/min.

2.4.4. *Pore structure analysis*

The pore structures of the investigated mixtures were evaluated using mercury intrusion porosimetry (Model: Antor Paar Poremaster). The total porosity and pore size distribution of the samples were determined. For each investigated mixture, about 1 g of samples with a size of roughly 5 × 5 × 5 mm were tested. The applied pressure ranged from 0.1 MPa to 400 MPa.

2.4.5. *Particle size distribution of $CaCO_3$ suspension*

The particle size distribution of the $CaCO_3$ suspensions was evaluated by a dynamic light scattering analyzer (Model: Zetasizer Nano ZS90). Two types of $CaCO_3$ suspensions prepared by the CI method and the CP method and diluted to 0.5% mass concentration, were used for the measurement.

2.4.6. *SEM-EDS analysis*

The distribution of $CaCO_3$ particles in the cement pastes was observed and analyzed using SEM and EDS. Samples with a size of 20 × 20 × 20 mm were cut from cube samples using a concrete saw after 28 days of curing. After 24 h of vacuum drying, the samples were then embedded in epoxy resin, dried for 24 h to harden, polished with silicon carbide papers, and dried for another 24 h before testing. The section of the cement pastes was observed by SEM at a magnification of 100x. Also, the element's carbon, which can represent the presence of $CaCO_3$ on the section, was mapped using EDS to visualize the distribution of $CaCO_3$ particles.

3. Experimental results and discussions

3.1. *Fresh and hardened properties*

3.1.1. *Flowability*

The mini-slump test results are shown in Fig. 2. For cement pastes prepared with CI-produced $CaCO_3$ suspensions, as the concentration of $CaCO_3$ increased from 0% to 6%, the mini-slump spread of fresh cement paste decreased from 250 mm to 193 mm (by 22.8%). For cement paste prepared with CP-produced $CaCO_3$ suspensions, as the concentration increased from 0% to 6%, the mini-slump spread of fresh cement paste decreased from 250 mm to 206 mm (by 17.6%). The reduction in flowability is because the nanoparticles with a high surface area absorbed free water on their outer layer (Ge et al., 2014). For mixtures with the same $CaCO_3$ concentration, the reduction in flowability by the CI method was slightly higher than that produced by the CP method, likely due to the finer particles and larger specific surface area of particles produced by the CI method.

3.1.2. *Compressive strength*

Fig. 3 presents the results of compressive strength of the investigated mixtures at 1, 3, and 28 days. For mixtures using CI-produced $CaCO_3$ suspensions, as the concentration increased from 0% to 1%, where $CaCO_3$ suspensions could be directly produced by CO_2 injection without additional processing, the compressive strength after 1 day increased from 33 MPa to 42 MPa (by 27%), and the compressive strength after 28 days increased from 50 MPa to 55 MPa (by 10%). As the concentration further increased from 1% to 6%, where mixtures were produced with the dilute-absorb-separate method, the 1-day compressive strength initially increased to 44 MPa (by 34% compared with the control mixture) at 2% concentration and then decreased to 40 MPa. The 28-day compressive strength initially increased to 58 MPa (by 16% compared with the control mixture) at 2% concentration and then decreased to 50 MPa. For mixtures using CP-produced $CaCO_3$ suspensions, as the concentration increased from 0% to 6%, the 1-day compressive strength initially increased from 33 MPa to 39 MPa (by 18%) at 4% $CaCO_3$ and then decreased to 49.5 MPa, and the 28-day compressive strength initially increased from 50 MPa to 54 MPa (by 8%) at 4% $CaCO_3$ and then decreased to 49 MPa.

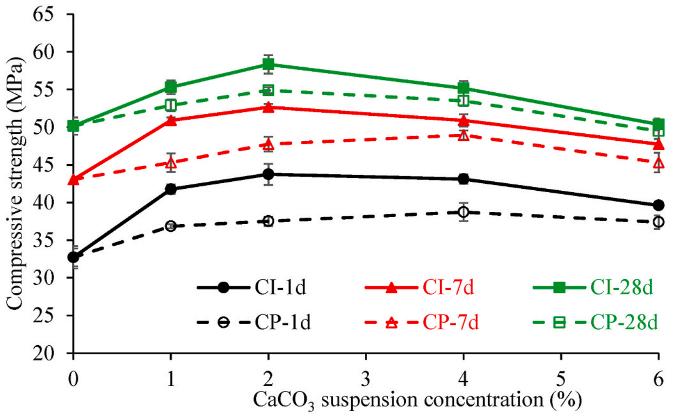

Fig. 3. Comparison of the compressive strengths of the mixtures prepared with the two methods for $CaCO_3$ suspensions.

At the same $CaCO_3$ concentration, the compressive strength of mixtures using CI-produced $CaCO_3$ is considerably higher than the mixtures using CP-produced $CaCO_3$. The 1-day compressive strength was highest at 2% for the CI method and 4% for the CP method, with the former value being 15% higher. This means that with 2% CI-produced $CaCO_3$ suspension, the compressive strength of the cement paste was 12% higher at 1 day and 8% higher at 28 days than that of the mixture with 4% CP-produced $CaCO_3$ suspension. This demonstrates the advantage of the CI method over the CP method in improving the mechanical properties of cementitious composites.

It was reported that the enhancement of mechanical properties is because the nano-$CaCO_3$ particles promote the hydration of the cement by providing extra seeding sites for the hydration products within the cement (Stefanidou and Papayianni, 2012). However, the difficulty of dispersion due to the high surface energy can limit the potential of these nanoparticles (Zhou et al., 2019). This could explain the compromise of the enhancement effect by both the CI and CP methods at concentrations higher than 2% and 4%, respectively. For CI-produced $CaCO_3$ suspension, the strength follows a decreasing trend as the concentration exceeds 2% because the degree of agglomeration of particles can increase during the sediment process. For CP-produced $CaCO_3$ suspension, the strength follows a decreasing trend as the concentration exceeds 4% because the particles are not well dispersed and can be easily agglomerated. Further, the CI method tends to contribute a more significant increase in strength compared to the CP method because the $CaCO_3$ particles generated by in-situ CO_2 injection are more well dispersed and homogeneous, which will be discussed in depth in the following sections.

3.2. *Effects of $CaCO_3$ suspensions on the hydration and microstructure of cement pastes*

3.2.1. *Hydration heat*

The hydration heat of the cement paste with 0%, 1%, and 4% $CaCO_3$ suspension produced by both the CI and CP methods is presented in Fig. 4. As shown in Fig. 4(a), the peak was earlier for all the mixtures using $CaCO_3$ suspension compared with the control mixture. The use of the 1% $CaCO_3$ suspension significantly increased the intensity of the heat peak. The increase of CaCO3 suspension concentration from 1% to 4% caused the main peak to occur earlier; however, the peak intensity was reduced. Compared with the cement paste prepared with CP-produced $CaCO_3$ suspensions at the same concentration, mixtures prepared with CI-produced $CaCO_3$ suspensions had peaks occurring earlier and with 5%–10% greater intensity. Multiple studies have proved that inactive nanoparticles can accelerate cement hydration (Stefanidou and Papayianni, 2012; Zhou et al., 2019; Huang et al., 2017) because the nanoparticles can behave as nuclei for the hydrates, and the grain boundary region was densely populated with nuclei and transformed completely early in the overall process of hydration (Wu et al., 2021). Fig. 4(b) shows the cumulative hydration heat at 48 h. In line with the heat flow results, the use of $CaCO_3$ suspension led to higher cumulative heat. However, with the concentration of nan0-$CaCO_3$ suspension increasing from 1% to 4%, the cumulative heat tended to be reduced after 24 h, leading to a reduction in total hydration heat in the first 48 h. This could be because agglomeration of particles compromised the nucleation effect, as well as the replacement of cement by $CaCO_3$, decreased some hydration reactions. These results indicate that incorporation of $CaCO_3$ by both the CI and CP methods can contribute to the hydration acceleration effect, where the CI method is more effective, and the effect can be compromised with an excessive amount of $CaCO_3$ due to the agglomeration.

3.2.2. *Phase development*

The development of the investigated cement pastes was evaluated after 28 days of curing using thermogravimetry analysis. Fig. 5(a) and Fig. 5(b) illustrate the weight change and differential weight change under rising temperatures for all mixtures. As the temperature increased from room temperature to 1000 °C, the mass monotonically decreased. This decrease is due to the vaporization and decomposition of hydration products. The differential weight change of each sample exhibited three peaks at temperatures 110 °C, 460 °C, and 660 °C, which can be attributed to the dehydration of C–S–H, ettringite, and AFm, the decomposition of $Ca(OH)_2$, and the decomposition of $CaCO_3$ respectively (Collodetti et al., 2014a). According to the mass changes in the ranges of 400–500 °C and 500–950 °C, the $CaCO_3$ and $Ca(OH)_2$ content were approximately calculated (Sargam and Wang, 2021). The results are presented in Fig. 5(c) and (d), respectively. For mixtures with CI-produced $CaCO_3$ suspensions, as the concentration increased from 0 to 4%, the content of $Ca(OH)_2$ increased from 14.2% to 15.8% (by 11%) at a 1% concentration and then decreased to 15.5%, and the content of $CaCO_3$ increased from 2.5% to 4.5%. For mixtures using CP-produced $CaCO_3$ suspensions, as the concentration increased from 0% to 4%, the content of $Ca(OH)_2$ increased from 14.2% to 15.2% (by 7.3%), and the content of $CaCO_3$ increased from 2.5% to 4.7%. The increase of $Ca(OH)_2$ content in mixtures using $CaCO_3$ suspensions is because of the cement hydration acceleration, and the trend of increase is in line with the hydration heat flow in Section 3.2.1. As for the $CaCO_3$ content, the increase in the composition was consistent with the increase in the concentration of the $CaCO_3$ suspension.

3.2.3. *Pore structure*

The pore structure characterized by cumulative and differential porosity at particle size from 1 nm to 10 μm for cement paste prepared without $CaCO_3$ suspension and with $CaCO_3$ suspension produced by the CI and CP methods are presented in Fig. 6.

In Fig. 6(a), the total porosity was substantially reduced in cement paste prepared with $CaCO_3$ suspension compared with the control mixture. For mixtures using CI-produced $CaCO_3$ suspensions, as the concentration increased from 0% to 4%, the total porosity initially decreased from 14.4% to 10.2% (by 29%) at 1% concentration, and then increased to 13.0%. For mixtures using CP-produced $CaCO_3$ suspensions, as the concentration increased from 0% to 4%, the total porosity decreased from 14.4% to 11.2% (by 22%) at 1% concentration, and then increased to 13.6%. CI method appeared to result in 8%–20% less porosity less than the CP method at the same $CaCO_3$ concentration. The porosity reduction of mixtures prepared by the CI method was more significant than that prepared by the CP method at the same concentration because of the better nucleation effects by $CaCO_3$ by the CI method, as is discussed in Section 3.2.1 and 3.2.2. Fig. 6(b) shows the differential pore size distribution. Compared with the control mixture, the peak intensity was weakened for all CI and CP mixtures. Also, the pore diameter of the peak was reduced from 100 nm to 15 nm (CI-1%), 20 nm (CP-1%), 40 nm (CI-4%), and 70 nm (CP-4%), which is because large pores become smaller due to the filler effect. There are three types of pores in cementitious materials: micropores, which are mainly gel pores (<10 nm), mesopores or capillary pores (10–5000 nm), and macropores due to deliberately entrained air or inadequate compaction (>5000 nm) (Meng and Khayat, 2018). It is known that pore size distribution is a key factor influencing the mechanical properties of concrete, in which capillary pores are responsible for the reduction of strength and durability (Zhang and Shao, 2018). In Fig. 6(b), total capillary pores were significantly reduced and shifted to pores of a smaller size for both CI and CP mixtures, and the reduction was greater for CI mixtures compared with CP mixtures at the same $CaCO_3$ suspension concentration. This can explain the trend of compressive strength changes and justify the advantage of the CI method in enhancing the mechanical properties of cement paste over the CP method.

3.3. *Discussion of the dispersion level of $CaCO_3$ suspensions prepared by CI and CP*

3.3.1. *Particle size distribution of $CaCO_3$ suspensions*

The $CaCO_3$ suspensions prepared using both the CI and CP methods were investigated in this section. The particle size distribution was measured after the suspension was freshly synthesized. To investigate the $CaCO_3$ particle dispersion change with time, which is important for

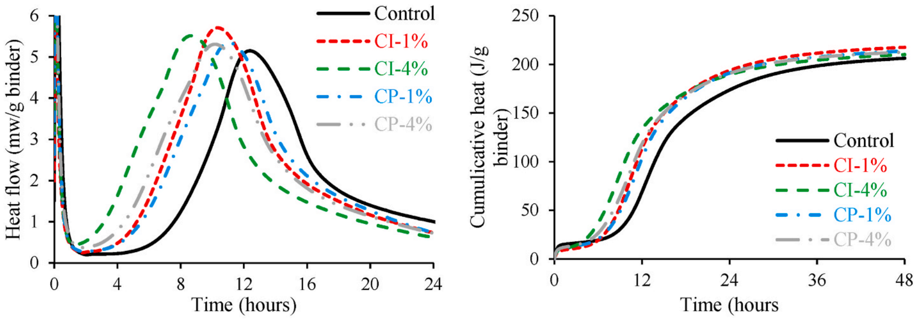

(a) (b)

Fig. 4. Hydration heat of investigated cement pastes: (a) heat flow, and (b) cumulative heat.

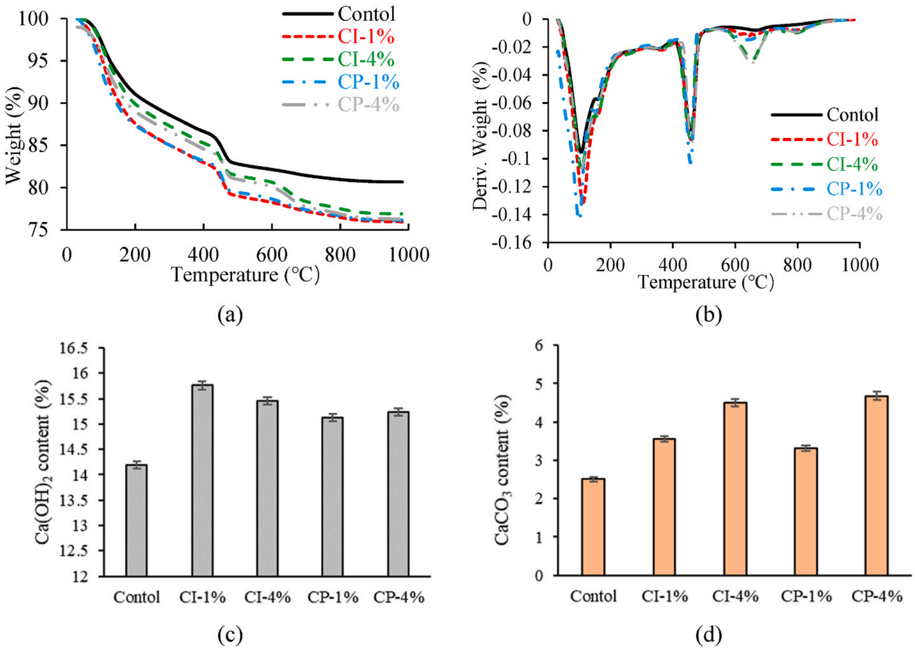

Fig. 5. Thermogravimetry analysis results of the investigated mixtures: (a) weight changes, (b) differential weight changes, (c) content of Ca(OH)$_2$, and (d) content of CaCO$_3$.

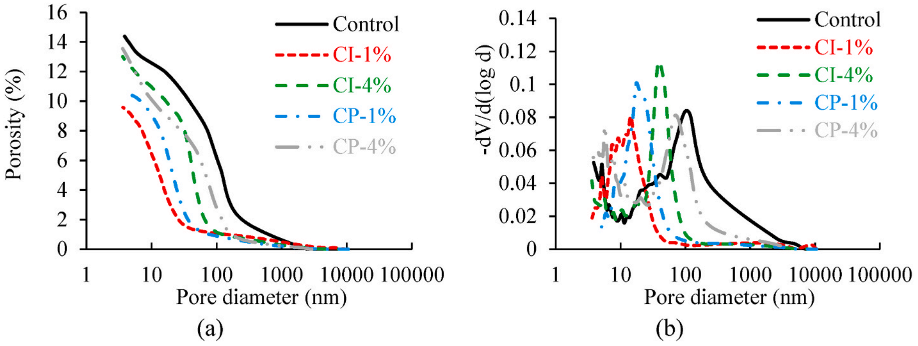

Fig. 6. Pore structure profile: (a) cumulative and (b) differential pore size distribution and (b) pore volume with various pore diameter ranges.

understanding the particle agglomeration behavior and guiding in-situ implementation, the measurement was also taken at 10 min and 30 min after the suspension was freshly synthesized. Also, both original suspensions prepared by the CP method and those dispersed by ultrasonic bath were measured. The suspending medium was water for ultrasonic dispersion treatments, and the treatments were applied for 15 min, using power levels of 30 W. The results of the particle size distributions are presented in Fig. 7. As can be seen from Fig. 7(a)**,** for CaCO$_3$ suspension produced by the CP method, the CaCO$_3$ suspension without ultrasonic dispersion has a mean particle size of 1500 nm, and the size of most of the particles is between 400 and 3000 nm, and a small amount of larger (4000–8000 nm) particles can also be identified. Considering that

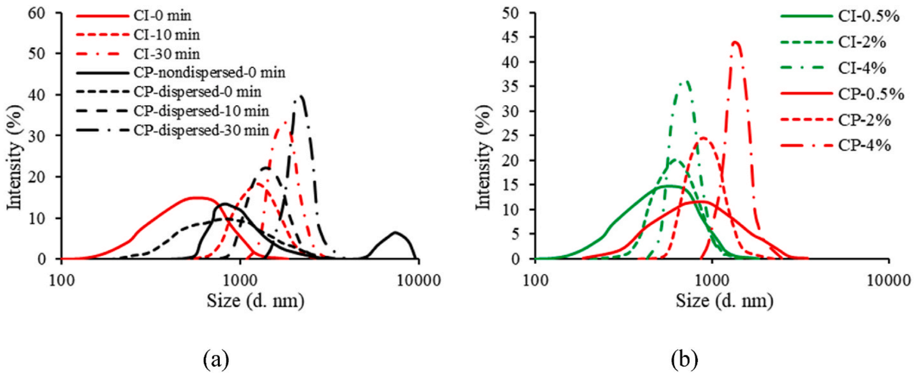

Fig. 7. Particle size distribution of CaCO$_3$ suspensions produced by the CI and CP methods: (a) changes with time, (b) changes with concentrations.

the diameter of nano-$CaCO_3$ powder is 30–60 nm, the result demonstrates that there are apparent agglomerates for $CaCO_3$ powder, which is a common phenomenon for nanomaterials and undermines its functionality in cementitious composites (Jin et al., 2013). With ultrasonic dispersion, the particle size of suspension at 0 min is reduced and is distributed continuously in a range of 200–4000 nm. The particle size grew with the increase in retention time after preparation, and the max-sized agglomerated particles were found around 4900 nm after 30 min. For the suspension produced by the CI method, the mean particle size was 600 nm, and most particles ranged between 100 and 1300 nm, showing nearly half the mean particle size compared with the fresh $CaCO_3$ suspension prepared by the CP method. Similarly, due to agglomeration, the particle size expands with the time after freshly synthesis, and the max-sized particles were observed around 3500 nm after 30 min of retention time. However, the mean size was noticeably lower than that of the CP counterpart. Better dispersion and homogeneity of the $CaCO_3$ particles in the suspensions produced by the CI method than those produced by the CP method with ultrasonic dispersion were also observed. In addition, as shown in Fig. 7(b), compared with the CP method, the CI method tends to generate $CaCO_3$ suspension with smaller sized particles for various concentration due to lower degree of agglomeration. Therefore, it can be expected that the $CaCO_3$ particles generated by CI method can be better distributed in the cementitious systems, which can enhance the filler effect and explain the better improvement in the mechanical properties of the cement pastes, as shown in Section 3.1.2. The results also imply that the nano-$CaCO_3$ particles will get agglomerated with time; this can justify the significance of adopting freshly synthesized $CaCO_3$ suspension for mixing cement-based materials that fully activate the filler effect of the nano-$CaCO_3$ particles in this study.

3.3.2. Dispersion analysis

3.3.2.1. SEM-EDS analysis. To verify the homogeneity of $CaCO_3$ particles in cement paste prepared using CI-produced $CaCO_3$ suspension within 1% concentration that showed significant enhancement for mechanical properties, SEM-EDS observations were conducted. As shown in Fig. 8(a) and Fig. 8(b), the white crystals existing on the sections of both the CI-1% and CP-1% samples were identified as $CaCO_3$ particles from the carbon mapping by EDS, as shown in Fig. 8(c) and (d). It is observed from the SEM images that the $CaCO_3$ particles in the CI-1% sample are finer and more well dispersed on the section than in the section of the CP-1% sample, where $CaCO_3$ particles are agglomerated in some areas. The mapping of carbon, which represents the locations of $CaCO_3$, can show this difference more clearly, as seen in the highlighted area in Fig. 8(d). This can justify the advantage of the CI method in dispersing the $CaCO_3$ particles and utilizing the potential of its nucleation effect to accelerate hydration and improve mechanical properties. This is because nanoparticles intrinsically tend to agglomerate because of the adhesion of particles to each other by van-der Waals forces (Collodetti et al., 2014b). Because the in-situ CI synthesized $CaCO_3$ is immediately used to mix with cement before they get agglomerated, the nano-$CaCO_3$ particles produced by this method can be evenly distributed in the cement paste and function as nucleation sites. In contrast, the dry nano-$CaCO_3$ powders produced by the CP method are already agglomerated to a certain degree when they are manufactured, transported, and stored.

3.3.2.2. Statistical analysis of $CaCO_3$ distribution. To further verify the SEM-EDS observations, we propose an alternative method to quantify the $CaCO_3$ distribution in cement paste, which is statistical analysis of $CaCO_3$ distribution in cement paste by measuring the $CaCO_3$ content in different parts of cement paste through TGA tests. Specifically, the quantification process are conducted as follows:

(i) Division of a section into multiple pieces

A paste slice cut from a cubic sample is divided into multiple pieces, specifically, a 20 mm × 20 mm x 2 mm sample is cut into 16 pieces marked as P1~P16, with each sample around 5 mm × 5 mm x 2 mm, as shown in below Fig. 9. Two groups of samples with one from CI-4% mixture and the other from CP-4% mixture are tested for comparison.

(ii) TGA quantification of $CaCO_3$ in each piece

Each piece is ground into powders and vacuum dried for 24h for TGA testing, around 50 mg powder is used for TGA, the test program is the same as described in Section 2.4.3, i.e. the powders were heated at a constant rate of 20 °C/min from 20 °C to 1000 °C in a nitrogen flow at a constant flow rate of 50 ml/min. Below Fig. 10 are the results showing the differential weight change under rising temperatures. The $CaCO_3$ contents are calculated according to mass changes at 500–900 °C corresponding to $CaCO_3$ decomposition.

(iii) Statistical analysis of TGA results

After obtaining the $CaCO_3$ contents of each piece in sample CI-4% and CP-4%, statistical analysis of the $CaCO_3$ distribution is conducted. Results for each piece and the average result and the standard deviation for each sample are summarized in below Table 4. To better present the homogeneity of $CaCO_3$ in cement paste, the data points of all pieces for each sample are shown in below Fig. 11, it is obvious that the data points for CI-4% sample are less dispersive than those for CP-4% sample. This is in accordance with the results obtained from SEM-EDS analysis, demonstrating that the CI method leads to better $CaCO_3$ dispersion level than the CP method.

4. Conclusion

This study investigated the effects of the proposed novel method, which injects CO_2 into cement-based materials, on the performance of cement-based materials. Cement pastes were prepared using the $CaCO_3$ suspension over a wide range of concentrations produced by this method, as well as a conventional method that directly incorporates nano-$CaCO_3$ powders.

Based on the above investigations, the following conclusions are drawn:

(1) $CaCO_3$ suspension can improve the compressive strength of cement pastes, and the strength gains increased with $CaCO_3$ concentration within a specific range and were compromised beyond that range. Compared with plain cement paste, 28-day compressive strength was increased by 16% by the CI method at an optimal concentration of 2% and by 8% by the CP method at an optimal concentration of 4%.

(2) Hydration heat kinetics and TGA both demonstrated that the cement hydration of cement paste prepared with $CaCO_3$ suspension was accelerated, and the CI method led to 5%–10% higher hydration heat and 2%–5% more hydration products than the CP method. MIP results revealed that the microstructures of cement paste prepared with $CaCO_3$ suspension were densified, and the CI method resulted in 8%–20% less porosity than the CP method.

(3) Particle size distribution analysis indicated that the CI method generated $CaCO_3$ suspension with a smaller particle size and a more uniform particle size distribution than the CP method. The SEM-EDS results showed that the distribution of $CaCO_3$ in CI-produced cement paste was more uniform than that of the CP reference. This can justify the better nucleation effect of nano-$CaCO_3$ particles using the CI method.

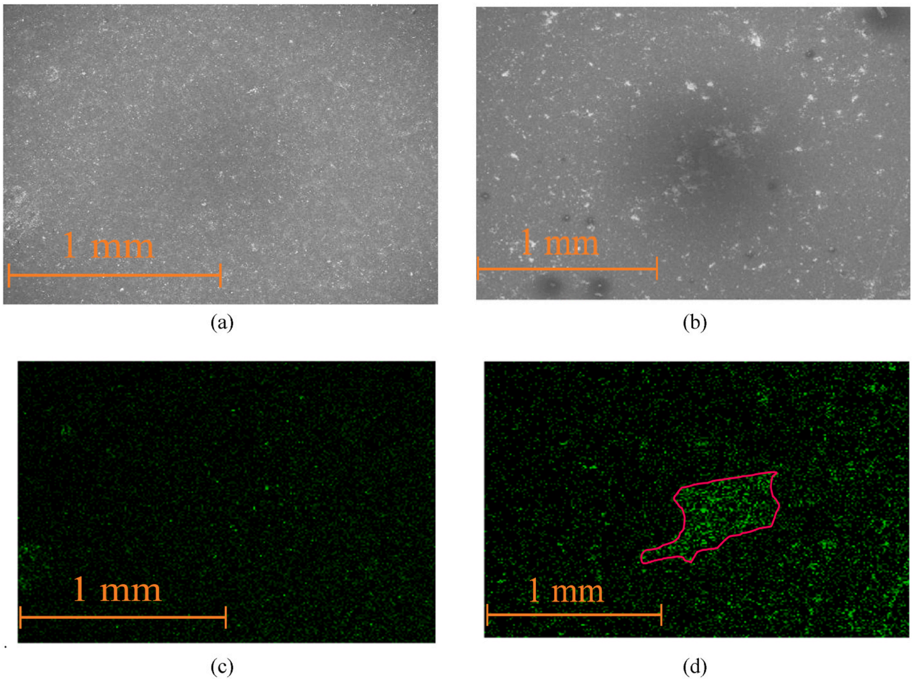

Fig. 8. SEM-EDS observation of mixture CI-1% and CP-1%: (a) SEM image of CI-1%, (b) SEM image of CP-1%, (c) carbon mapping of CI-1%, and (d) carbon mapping of CP-1%.

P1	P2	P3	P4
P5	P6	P7	P8
P9	P10	P11	P12
P13	P14	P15	P16

Fig. 9. TGA analysis on solid separated from the carbonated suspension.

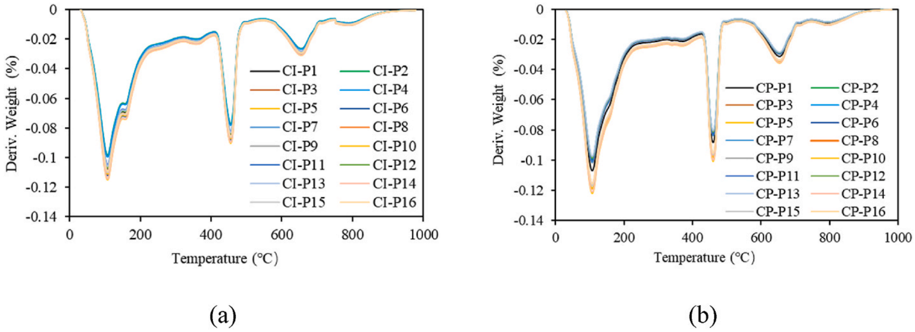

Fig. 10. Differential weight changes of samples under rising temperatures: (a) mixture CI-4%, (b) mixture CP-4%.

CRediT authorship contribution statement

Zhuo Liu: Validation, Investigation, Data curation, Writing – original draft, Visualization. **Jiang Du:** Investigation, Writing – review & editing. **Weina Meng:** Conceptualization, Methodology, Resources, Writing – review & editing, Supervision, Project administration, Funding acquisition.

Declaration of competing interest

The authors declare that they have no known competing financial interests or personal relationships that could have appeared to influence

Table 4
$CaCO_3$ content statistics for sample CI-4% and CP-4%.

		$CaCO_3$ content (%)				
CI-4%	P1-4	4.68	4.45	4.54	4.31	Avg = 4.67
	P5-8	4.99	4.87	4.5864	4.54	Std = 0.19
	P9-12	4.73	4.82	4.54	4.63	
	P13-16	4.59	4.96	4.77	4.73	
CP-4%	P1-4	4.87	4.62	4.41	4.18	Avg = 4.74
	P5-8	5.34	5.21	4.31	4.27	Std = 0.44
	P9-12	5.06	5.21	4.27	4.31	
	P13-16	4.27	5.31	5.11	5.06	

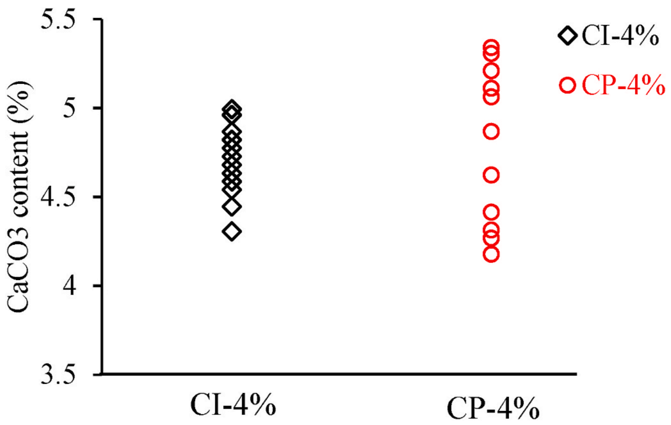

Fig. 11. $CaCO_3$ content data points of all pieces for both samples.

the work reported in this paper.

Data availability

Data will be made available on request.

Acknowledgments

This research was funded by the National Science Foundation (grant number: CMMI 2046407) and the New Jersey Department of Transportation-funded Task Order 388 – Bridge Resource Program 2021–2021 RIME, Contract ID Number: 21–5086.

References

Ashraf, W., 2016. Carbonation of cement-based materials: challenges and opportunities. Construct. Build. Mater. 120, 558–570.
Ashraf, W., Olek, J., Sahu, S., 2019. Phase evolution and strength development during carbonation of low-lime calcium silicate cement (CSC). Construct. Build. Mater. 210, 473–482.
Batuecasa, E., Liendob, F., Tommasi, T., Bensaid, S., Deorsola, F.A., Fino, D., 2021. Recycling CO_2 from flue gas for $CaCO_3$ nanoparticles production as cement filler: a Life Cycle Assessment. J. CO2 Util. 45, 101446.
Bodansky, D., 2016. The legal character of the Paris Agreement. Rev. European, Comparat. Int. Environ. Law 25 (2), 142–150.
Camiletti, J., Soliman, A., Nehdi, M., 2013. Effects of nano-and micro-limestone addition on early-age properties of ultra-high-performance concrete. Mater. Struct. 46 (6), 881–898.
Chen, T., Gao, X., 2019. Effect of carbonation curing regime on strength and microstructure of portland cement paste. J. CO2 Util. 34, 74–86.
Collodetti, G., Gleize, P.J., Monteiro, P.J., 2014a. Exploring the potential of siloxane surface modified nano-SiO_2 to improve the portland cement pastes hydration properties. Construct. Build. Mater. 54, 99–105.
Collodetti, G., Gleize, P.J., Monteiro, P.J., 2014b. Exploring the potential of siloxane surface modified nano-SiO_2 to improve the portland cement pastes hydration properties. Construct. Build. Mater. 54, 99–105.
Di Maria, A., Snellings, R., Alaerts, L., Quaghebeur, M., Van Acker, K., 2020. Environmental assessment of CO_2 mineralisation for sustainable construction materials. Int. J. Greenh. Gas Control 93.
Ge, Z., Wang, K., Sun, R., Huang, D., Hu, Y., 2014. Properties of self-consolidating concrete containing nano- $CaCO_3$. J. Sustain. Cement-Based Mater. 3 (3–4), 191–200.
Godin, J., Liu, W., Ren, S., Xu, C., 2021a. Advances in recovery and utilization of carbon dioxide: a brief review. J. Environ. Chem. Eng. 9 (4), 105644.
Godin, J., Liu, W., Ren, S., Xu, C.C., 2021b. Advances in recovery and utilization of carbon dioxide: a brief review. J. Environ. Chem. Eng. 9 (4), 105644.
Han, S.-J., Yoo, M., Kim, D.-W., Wee, J.-H., 2011. Carbon dioxide capture using calcium hydroxide aqueous solution as the absorbent. Energy Fuel. 25 (8), 3825–3834.
Hepburn, C., Adlen, E., Beddington, J., Carter, E.A., Fuss, S., Mac Dowell, N., Minx, J.C., Smith, P., Williams, C.K., 2019. The technological and economic prospects for CO_2 utilization and removal. Nature 575 (7781), 87–97.
Ho, H., Iizuka, A., Shibata, E., Tomita, H., Takano, K., Endo, T., 2021. Utilization of CO_2 in direct aqueous carbonation of concrete fines generated from aggregate recycling: influences of the solid–liquid ratio and CO_2 concentration. J. Clean. Prod. 312, 127832.
Huang, W., Kazemi-Kamyab, H., Sun, W., Scrivener, K., 2017. Effect of cement substitution by limestone on the hydration and microstructural development of ultra-high performance concrete (UHPC). Cement Concr. Compos. 77, 86–101.
Jin, S., Zhang, J., Han, S., 2013. Relationship between compressive strength and fractal dimension of pore structure. Rare Met. Mater. Eng. 42 (12), 2433–2436.
Karl, T.R., Trenberth, K.E., 2003. Modern global climate change. Science 302 (5651), 1719–1723.
Kawashima, S., Hou, P., Corr, D.J., Shah, S.P., 2013. Modification of cement-based materials with nanoparticles. Cement Concr. Compos. 36, 8–15.
Kawashima, S., Seo, J.-W.T., Corr, D., Hersam, M.C., Shah, S.P., 2014. Dispersion of $CaCO_3$ nanoparticles by sonication and surfactant treatment for application in fly ash–cement systems. Mater. Struct. 47 (6), 1011–1023.
Lempert, R., Preston, B.L., Edmonds, J., Clarke, L., Wild, T., Binsted, M., Diringer, E., Townsend, B., 2019. Pathways to 2050. Center for Climate Energy Solutions.
Liew, M.S., Nguyen-Tri, P., Nguyen, T.A., Kakooei, S., 2019. Smart Nanoconcretes and Cement-Based Materials: Properties, Modelling and Applications. Elsevier.
Liu, Z., Meng, W., 2021. Fundamental understanding of carbonation curing and durability of carbonation-cured cement-based composites: a review. J. CO2 Util. 44, 101428.
Liu, X., Zhou, J., Zhang, Y., Liu, X., Chen, Y., Yong, X., Wang, S., Zheng, T., Yuan, H., 2015. Continuous process of biogas purification and co-production of nano calcium carbonate in multistage membrane reactors. Chem. Eng. J. 271, 223–231.
Lu, B., Shi, C., Cao, Z., Guo, M., Zheng, J., 2019. Effect of carbonated coarse recycled concrete aggregate on the properties and microstructure of recycled concrete. J. Clean. Prod. 233, 421–428.
Meng, W., Khayat, K.H., 2018. Effect of graphite nanoplatelets and carbon nanofibers on rheology, hydration, shrinkage, mechanical properties, and microstructure of UHPC. Cement Concr. Res. 105, 64–71.
Monkman, S., MacDonald, M., 2016. Carbon dioxide upcycling into industrially produced concrete blocks. Construct. Build. Mater. 124, 127–132.
Monkman, S., MacDonald, M., 2017. On carbon dioxide utilization as a means to improve the sustainability of ready-mixed concrete. J. Clean. Prod. 167, 365–375.
Monkman, S., MacDonald, M., Hooton, R.D., Sandberg, P., 2016. Properties and durability of concrete produced using CO_2 as an accelerating admixture. Cement Concr. Compos. 74, 218–224.
Norhasyima, R.S., Mahlia, T.M.I., 2018. Advances in CO_2 utilization technology: a patent landscape review. J. CO2 Util. 26, 323–335.
Østergaard, P.A., Johannsen, R.M., Duic, N., 2020. Sustainable development using renewable energy systems. Int. J. Sustain. Energy Plan. Manag. 29, 1–6.
Pan, X., Shi, C., Hu, X., Ou, Z., 2017. Effects of CO_2 surface treatment on strength and permeability of one-day-aged cement mortar. Construct. Build. Mater. 154, 1087–1095.
Qian, X., Wang, J., Fang, Y., Wang, L., 2018. Carbon dioxide as an admixture for better performance of OPC-based concrete. J. CO2 Util. 25, 31–38.
Raki, L., Beaudoin, J., Alizadeh, R., Makar, J., Sato, T., 2010. Cement and concrete nanoscience and nanotechnology. Materials 3 (2), 918–942.
Raza, A., Gholami, R., Rezaee, R., Rasouli, V., Rabiei, M., 2019a. Significant aspects of carbon capture and storage–a review. Petroleum 5 (4), 335–340.
Raza, A., Gholami, R., Rezaee, R., Rasouli, V., Rabiei, M., 2019b. Significant aspects of carbon capture and storage – a review. Petroleum 5 (4), 335–340.
Ritchie, H., Roser, M., 2020. CO_2 and Greenhouse Gas Emissions. Our World in Data.
Salvia, M., Reckien, D., Pietrapertosa, F., Eckersley, P., Spyridaki, N.-A., Krook-Riekkola, A., Olazabal, M., Hurtado, S.D.G., Simoes, S.G., Geneletti, D., 2021. Will climate mitigation ambitions lead to carbon neutrality? An analysis of the local-level plans of 327 cities in the eu. Renew. Sustain. Energy Rev. 135, 110253.
Sargam, Y., Wang, K., 2021. Quantifying dispersion of nanosilica in hardened cement matrix using a novel sem-eds and image analysis-based methodology. Cement Concr. Res. 147, 106524.
Šavija, B., Luković, M., 2016. Carbonation of cement paste: understanding, challenges, and opportunities. Construct. Build. Mater. 117, 285–301.
Schreyer, F., Luderer, G., Rodrigues, R., Pietzcker, R.C., Baumstark, L., Sugiyama, M., Brecha, R.J., Ueckerdt, F., 2020. Common but differentiated leadership: strategies and challenges for carbon neutrality by 2050 across industrialized economies. Environ. Res. Lett. 15 (11), 114016.
Stefanidou, M., Papayianni, I., 2012. Influence of nano-SiO_2 on the portland cement pastes. Compos. B Eng. 43 (6), 2706–2710.
Stuardi, F.M., MacPherson, F., Leclaire, J., 2019. Integrated CO_2 capture and utilization: a priority research direction. Current Opinion Green Sustain. Chem. 16, 71–76.
Su, Y., Li, J., Wu, C., Wu, P., Li, Z.-X., 2016. Influences of nano-particles on dynamic strength of ultra-high performance concrete. Compos. B Eng. 91, 595–609.
Wu, Z., Shi, C., Khayat, K.H., 2018. Multi-scale investigation of microstructure, fiber pullout behavior, and mechanical properties of ultra-high performance concrete with nano-$CaCO_3$ particles. Cement Concr. Compos. 86, p255–p265.

Wu, Z., Khayat, K.H., Shi, C., Tutikian, B.F., Chen, Q., 2021. Mechanisms underlying the strength enhancement of UHPC modified with nano-SiO2 and nano-$CaCO_3$. Cement Concr. Compos. 119, 103992.

Xu, Z., Zhou, Z., Du, P., Cheng, X., 2017. Effects of nano-limestone on hydration properties of tricalcium silicate. J. Therm. Anal. Calorim. 129 (1), 75–83.

Yang, H., Che, Y., 2018. Effects of nano-$CaCO_3$/limestone composite particles on the hydration products and pore structure of cementitious materials. Adv. Mater. Sci. Eng. 2018.

Yeşilmen, S., Al-Najjar, Y., Balav, M.H., Şahmaran, M., Yıldırım, G., Lachemi, M., 2015. Nano-modification to improve the ductility of cementitious composites. Cement Concr. Res. 76, 170–179.

Zhang, D., Shao, Y., 2018. Surface scaling of CO_2-cured concrete exposed to freeze-thaw cycles. J. CO2 Util. 27, p137–p144.

Zhang, Y., Li, S., Luo, T., Gao, J., 2020a. The effect of emission trading policy on carbon emission reduction: evidence from an integrated study of pilot regions in China. J. Clean. Prod. 265, 121843.

Zhang, Z., Pan, S.-Y., Li, H., Cai, J., Olabi, A.G., Anthony, E.J., Manovic, V., 2020b. Recent advances in carbon dioxide utilization. Renew. Sustain. Energy Rev. 125, 109799.

Zhang, Z., Pan, S.-Y., Li, H., Cai, J., Olabi, A.G., Anthony, E.J., Manovic, V., 2020c. Recent advances in carbon dioxide utilization. Renew. Sustain. Energy Rev. 125.

Zhou, J., Zheng, K., Liu, Z., He, F., 2019. Chemical effect of nano-alumina on early-age hydration of portland cement. Cement Concr. Res. 116, 159–167.